Available online at www.sciencedirect.com
ScienceDirect
International Journal of Heat and Mass Transfer 51 (2008) 2444–2454
International Journal of HEAT and MASS TRANSFER
www.elsevier.com/locate/ijhmt

Classification of turbulent jets in a T-junction area with a 90-deg bend upstream

Seyed Mohammad Hosseini *, Kazuhisa Yuki, Hidetoshi Hashizume

QSE Department, Tohoku University, Aoba-Ku, Sendai 980-8579, Japan

Received 6 November 2006; received in revised form 11 July 2007
Available online 22 October 2007

Abstract

Many nuclear power plants report high cycle thermal fatigue in their cooling system, which is caused by temperature fluctuation in a non-isothermal mixing area. One of these areas is the T-junction, in which fluids of various temperatures and velocities blend. The objective of this research is to classify the turbulent jet mechanics in order to examine the flow-field structure under various operating conditions. Furthermore, this research discovers the optimum operating conditions of the mixing tee in this piping system. An experimental model, including the T-junction with a 90-deg bend upstream, is operated to analyze this mixing phenomenon based on the real operation design of the Phenix reactor. The temperature and velocity data show that a 90-deg bend has a strong effect on the fluid mixing mechanism and the momentum ratio between the main velocity and the branch velocity of the T-junction, which could be an important parameter for the classification of the fluid mixing mechanism. By comparing their mean velocity distributions, velocity fluctuations, and time-series data, the behavior of the branch jet is categorized into four types of turbulent jets; sorted from the highest to the lowest momentum ratios, the jets are categorized as follows: the wall jet, the re-attached jet, the turn jet, and the impinging jet. Ultimately, the momentum ration of the turn jet was selected as the optimum operating condition because it has the lowest velocity and the lowest temperature fluctuations near the wall of the mixing tee.

Keywords: Turbulent jet; T-junction; PIV; Piping system

1. Introduction

Thermal stress arising from temperature fluctuations in the cooling system of nuclear power plants is inevitable. When thermal stress is generated by a sudden change in temperature, the process is referred to as thermal shock; failure under repetitive application of thermal stress has been termed thermal fatigue. The severity of the failure is dependent on the shape of the component, the fluid mixing mechanism, and the temperature distribution. Studies of thermal fatigue in power plants were initially carried out for liquid-metal-cooled fast breeder reactors because of the high thermal conductivity of liquid-metal coolants. After many recent thermal fatigue events occurred in various nuclear power plants, such as the French PWR CIVAX in 1998, the Japanese PWR Tsuruga-2 in 1999, the Japanese PWR Tomari-2 in 2003, the focus of thermal striping studies shifted to not only fast breeder reactors but also light water reactors. The T-junction, was selected because it is a component common to the cooling systems of most nuclear power plants that has a high capability of thermal fatigue. Several types of numerical and experimental research has been performed based on the fluid mixing phenomena in the T-junction, such as the evaluation of thermal fatigue [1], the numerical simulation of the mixing phenomenon [2], and the analysis of the flow-field structure [3], all of which considered the T-junction as a single component. Although the T-junction has typically been considered a single component, the mixing tee is usually connected to another part of the complex piping

* Corresponding author. Tel./fax: +81 22 7957906.
E-mail address: hoseini@karma.qse.tohoku.ac.jp (S.M. Hosseini).

0017-9310/$ - see front matter © 2007 Elsevier Ltd. All rights reserved.
doi:10.1016/j.ijheatmasstransfer.2007.08.024

Nomenclature

C	constant number
C_R	curvature ratio
D_b	branch pipe diameter
D_m	main pipe diameter
d	distance between bend and branch pipe
E	secondary flow energy
E_{mean}	mean flow energy
I	intensity of the velocity fluctuation
I_{max}	maximum velocity fluctuation
M_b	branch flow momentum
M_m	main flow momentum
M_R	momentum ratio
m	sampling number of measurement
n	frame number
Q_b	branch flow rate
Q_m	main flow rate
s_j	standard deviation in a j direction
s_r	radial velocity standard deviation
s_z	axial velocity standard deviation
T_{branch}	temperature of branch flow
T_{main}	temperature of main flow
T_i	instantaneous temperature
T_m	mean temperature
ΔT	temperature difference
ΔT_{rms}	temperature fluctuation intensity
T_{P-P}	pick to pick temperature variation
t	time separation
U	mean velocity
U_{ave}	average of absolute velocity
U_b	branch velocity
U_m	main velocity
U_{max}	maximum velocity
$u_{j,i}$	velocity at i frame in a j direction
$\overline{u_j}$	average velocity in a j direction
$u_{r,i}$	radial velocity at i frame
$u_{z,i}$	axial velocity at i frame
z	longitudinal distance along axial direction
ρ_b	branch flow density
ρ_m	main flow density

system—one of these parts is a 90-deg bend that typically exists upstream of the T-junction and has strong effects on the mixing mechanism [4,5].

The particle image velocimetry (PIV) technique and the thermocouple network were used to experimentally investigate the fluid mixing phenomenon in the T-junction area with the 90-deg bend upstream [6–8]. It is difficult to fully understand the heat transport mechanism of fluid toward the wall through the mere visualization of the entire flow-field, therefore a small region around the jet nozzle was selected to more easily measure close-up flow-field data (the thermocouples are installed on this same region's main pipe wall). This visualization displays origins of the velocity fluctuations in the T-junction area.

The thermo-hydraulic characteristics of the turbulent jet are analyzed to better classify the fluid mixing mechanism. This classification is important factor to categorize operating conditions and estimate the effects of thermal fatigue in each mixing condition in the piping system.

According to the strong effects of the 90-deg bend on the fluid mixing mechanism, two parameters that essentially control the behavior of bend, such as curvature ratio of the bend and axial distance between the bend and T-junction area, are selected. On the other hand, the momentum ratio between the main velocity and the branch velocity of the mixing tee is a most useful parameter for classifying the fluid mixing mechanism, which includes both the velocity and pipe diameter characteristics of the main and branch pipes. In addition, the effects of velocity and pipe diameter on the fluid mixing mechanism are investigated separately to explain the behavior of turbulent jets and the different operating conditions caused by each term of the bend. Finally, depending on the flow velocity, pipe diameter, and fluid temperature of the branch and main flows, four different jets exist: the wall jet, re-attached jet, turn jet and impinging jet. These jets have different mixing mechanisms in the T-junction area, which determine their suitability for prolong operations in the cooling system of various power plants.

2. Experimental apparatuses

The fluid cycle system and T-junction area are shown in Fig. 1. Both the main and branch pipes are made of 3 mm thick acrylic circular pipes, and the branch pipe is connected to the main pipe at right angle to form the mixing tee with a square-edge. The internal main pipe diameter, D_m, is 108 mm and the branch pipe can have three different diameters, either $D_b = 15$, 21 or 31 mm. The main pipe runs vertically upward in the test section, which is connected to a measuring window downstream for visualizing lateral flow-field. A 90-deg bend is installed upstream of the T-junction. This bend is stainless steel with a 1.41 curvature ratio. The main flow is straightened by a reducer, a long main pipe before the 90-deg bend ($13D_m$), and a straightener tank, made from acrylic plates with $30 \times 30 \times 30\ cm^3$ size. The branch pipe also is long enough ($60D_b$) to inject fully developed flow into the mixing area.

A heat-exchanger and a heating tank are used to control the inlet temperature of both the main flow and branch flow in the mixing tee. They are respectively set behind the mixing tank and the branch pump. The heat-exchanger has a secondary cooling system for decreasing the temperature with city water, and its flow rate is controlled by an

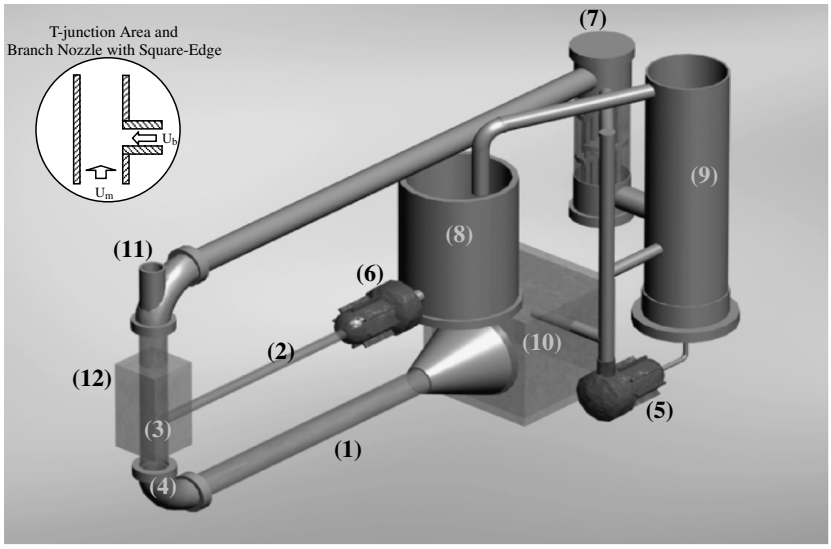

Fig. 1. Experimental apparatuses.

inlet heat-exchanger valve. Whereas, the heating tank uses gas and electric heaters to warm the branch flow.

The mixing tank is positioned in order to insert small tracers and remove bubbles from the main cycle. This tank is linked to other apparatuses by five pipe connections (the heat-exchanger pipe, emergency inlet pipe, heating tank pipe, main pump pipe and draying outlet pipe). There are two main and branch pumps with 600 and 75 L/min maximum flow rates. A flow rate control valve and an inverter individually adjust the mean velocity of these flows. There is a cube water jacket around the T-junction area, which is made of the same acrylic plates as the piping material to decrease the effect of the laser light's refraction through the circular pipe wall during the visualization of longitudinal sections.

3. Experimental conditions and analysis methods

Water was the only working fluid in the experimental loop throughout this research. The PIV system is used to visualize the flow characteristics in the T-junction area. Two conditions are selected to visualize the flow-field—the whole flow-field (long-shot) and the close-up flow-field with 150 mm × 150 mm and 60 mm × 60 mm view sections, respectively. The resolution of each section is 1018 × 1008 pixels. The interrogation cell is divided into 64 × 64 pixels at each segment for measuring the whole flow-field and 32 × 32 pixels for measuring a close-up area with 50% area overlap and 100 μs time interval. The cross-section is visualized into the radial and axial velocity matrixes ($u_{r,i}$ and $u_{z,i}$). Both matrixes have 30 × 29 arrays when 64 × 64 pixels are cross-correlated, and have 62 × 59 arrays when 32 × 32 pixels cross-correlations are used. Laser sheet thickness is 1–3 mm, with a 200 mJ energy level; this width is selected based on the three parameters, the visualization area, amount of tracer in the fluid and distance between the visualization cross-section and the camera lens. Two kinds of tracers with different diameters are used, both made from nylon powder with 1.03 g/cm^3 density. The tracer with an 80 μm diameter is used for visualizing the whole flow-field and a 20 μm diameter for the close-up flow-field condition. The camera starts shooting with 30 Hz frequency, which has a frame rate of 30 fps, in triggered double exposure mode; each shot continually captures 99 images. Forty-nine velocity vector maps are obtained with only 0.03 s time gaps. Five shots are taken, and in total, 240 frames are used to evaluate both flow-fields. The visualization of horizontal and vertical areas is shown in Fig. 2.

Average flow-field and intensity of velocity fluctuation are evaluated by the following equations:

$$U_{\text{ave}} = \frac{1}{n}\sum_{i}^{n}\sqrt{(u_{r,i}^2 + u_{z,i}^2)}, \tag{1}$$

$$s_j = \left(\frac{1}{n}\sum_{i=1}^{n}(u_{j,i} - \overline{u_j})^2\right)^{1/2}, \tag{2}$$

$$U_{\text{mix}} = \sqrt{(U_b^2 + U_m^2)}, \tag{3}$$

$$I = \sqrt{(s_r^2 + s_z^2)/2}/U_{\text{mix}}, \tag{4}$$

where $u_{r,i}$ and $u_{z,i}$ represent the instantaneous radial and axial velocities at the i frame, and U_{ave} is the averaged absolute velocity, and n is the total number of the frames. U_b and U_m represent both the branch and main velocities. s_r and s_z are standard deviations of the velocity variation in the radial and axial directions. Lastly, I represents the intensity of velocity fluctuation.

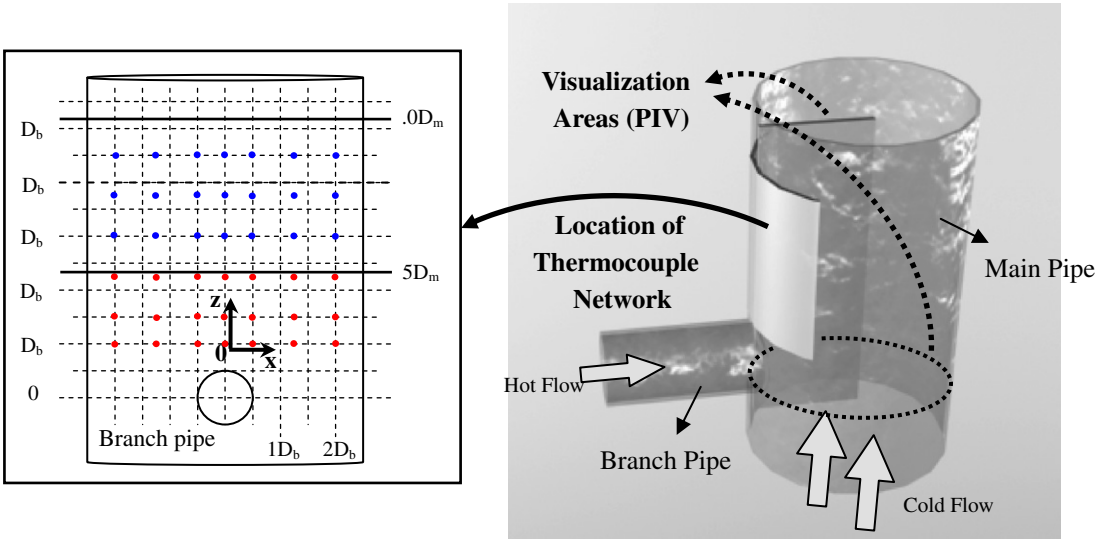

Fig. 2. Locations of the thermocouple network and PIV visualization areas.

To measure the temperature of fluid in the vicinity of the main pipe in the T-junction area above the branch pipe, 42 thermocouples were installed 1 mm from the wall, and this area was covered by a heat insulator. The positions of the thermocouple are shown in Fig. 2. Here, both the main and branch flows are entirely in the turbulent regime.

The temperature fluctuation intensity, ΔT_{rms}, is calculated at each measuring point from the time-series temperature data and is normalized by using the following equations:

$$\Delta T = T_{branch} - T_{main}, \tag{5}$$

$$\Delta T_{rms} = \left(\sqrt{\sum (T_i - T_m)^2/m}\right)/\Delta T, \tag{6}$$

where T_i and T_m represent instantaneous temperature and mean temperature, ΔT is the temperature difference between two fluids, and m is total sampling number of the temperature data.

4. Results and discussion

4.1. Classification of turbulent jets

Turbulent jets in finite space show various behaviors, one of these finite spaces is the T-junction area which two pipes with different diameters and flow are connected together at right angle with a square-edge. Based on the velocity and momentum ratio of these pipes, the flow pattern in the mixing tee area has different mechanisms, thus many turbulent jets exist. The other parameters used to categorized mixing mechanism are Reynolds number of the branch pipe and Dean number of the main pipe, which are more complicated than the momentum ratio, therefore, they do not show a clear classification of the jets.

Depending on the momentum/velocity ratio of the entering flows from branch pipe and the main pipe, the turbulent mixing patterns can be further divided into four branch jets such as the wall jet, re-attached jet, turn jet and impinging jet. The types of mixing flow are categorized by using the momentum ratio equation as follows:

$$M_R = \frac{\rho_m U_m^2 \cdot (D_m \times D_b)}{\rho_b U_b^2 \cdot \pi \cdot (D_b/2)^2}, \tag{7}$$

M_R is the momentum ratio, ρ_m and ρ_b are the fluid densities for the main flow and branch flow, U_m and U_b are the mean velocity of the main and branch flow, D_m and D_b are the main and branch pipe diameters.

For distinguishing these four jets in the flow pattern, we need a basic introduction of each jet and some parameters to distinguish each group. Three parameters are used to investigate their structures and mechanisms: mean velocity distribution, velocity fluctuation and time-series data (see Figs. 3–6). Attending to these parameters, the branch jets are separated by mean velocity distribution and velocity fluctuation. The mean velocity distribution contains information about the average structure of the jet, while, the velocity fluctuations display the area with highest variation. In the next step, the time-series data of each condition are investigated to explain the gradual change of the temporal flow structure. For each condition, 240 frames are used to evaluate the mixing flow mechanism; the first three frames from each condition are shown in Figs. 3–6. Finally, all jets are classified into the aforementioned categories based on the shape and behavior of the branch jets. For providing exact investigation method of these jets, the structure and mechanism of each jet are described separately:

(a) Wall jet: The wall jet is characterized by a higher main flow and a lower branch flow. Here, the jet does not separate from the main pipe wall. Velocity fluctuations occur only near the wall of main pipe as shown in Fig. 3.

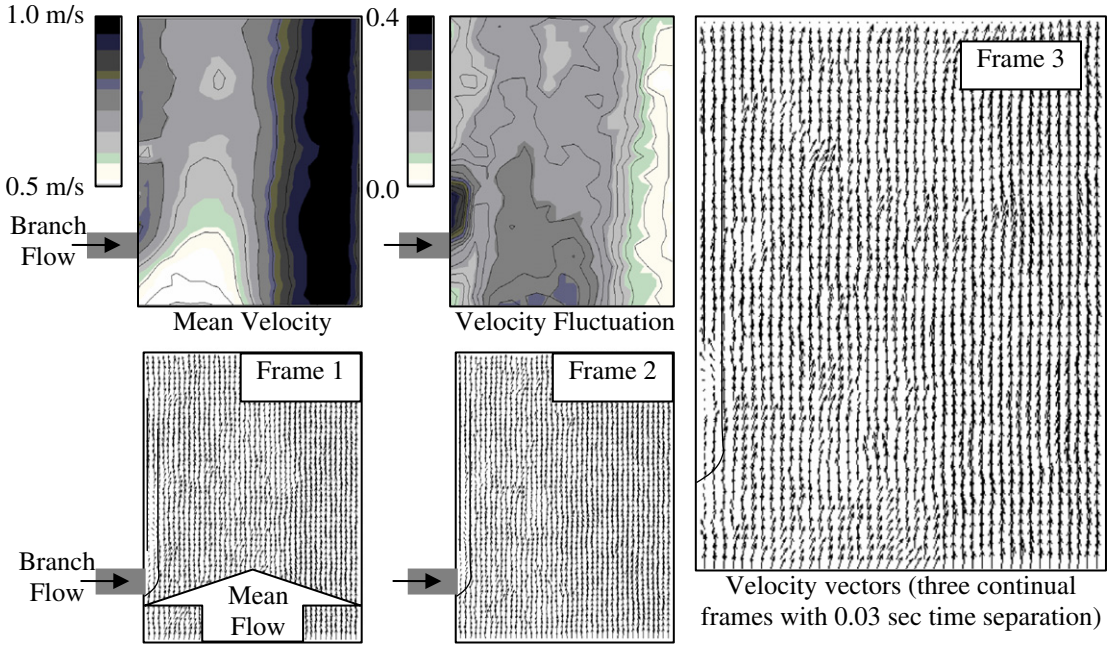

Fig. 3. Wall jet ($D_m = 108$ mm, $D_b = 15$ mm, $U_m = 0.89$ m/s, $U_b = 0.22$ m/s).

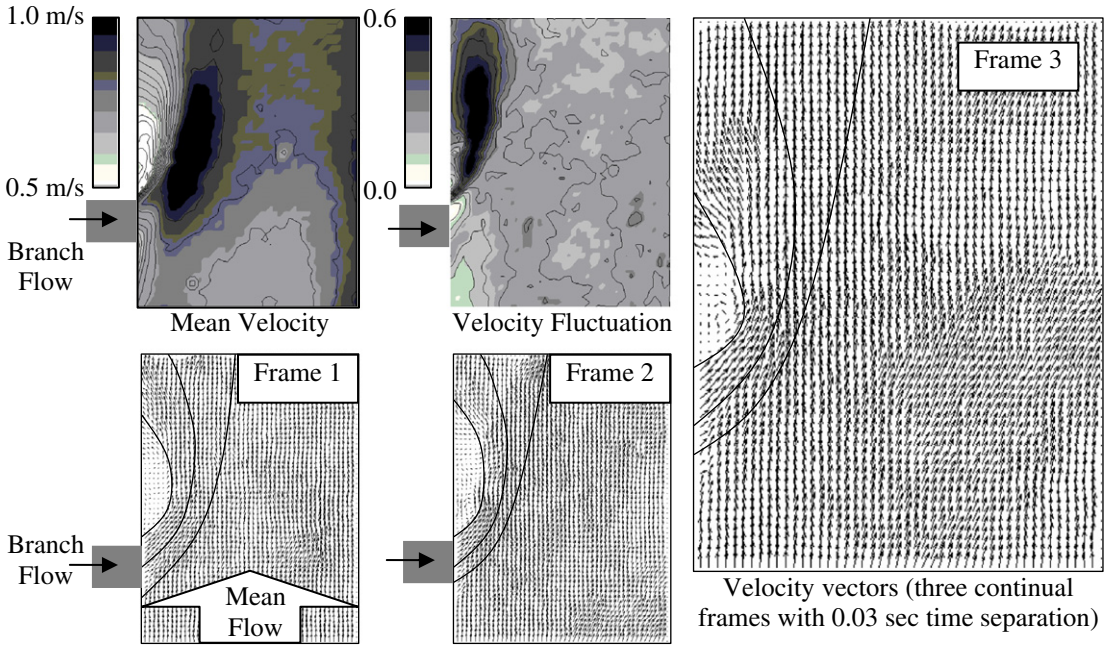

Fig. 4. Re-attached jet ($D_m = 108$ mm, $D_b = 21$ mm, $U_m = 0.89$ m/s, $U_b = 0.23$ m/s).

(b) Re-attached jet: The re-attached jet is distinguished by an interaction between the secondary flow of the main pipe and the branch flow. The branch jet turns to the center axis of the main pipe and then turns again to the main pipe wall above the branch nozzle in Fig. 4.

(c) Turn jet: The turn jet exists when two inlet flows have comparable momentums, and the branch jet turns to the center axis of the main pipe in the same direction as the main flow provided in Fig. 5.

(d) Impinging jet: The impinging jet occurs when the branch velocity is much higher than the main velocity, and as a result, the branch flow can touch the opposite wall of the main pipe as visualized in Fig. 6.

According to the momentum/velocity ratios between the branch and main flow, three branch pipe diameters were used to categorize branch jets. In order to categorize flow patterns, 205 conditions were selected. Each

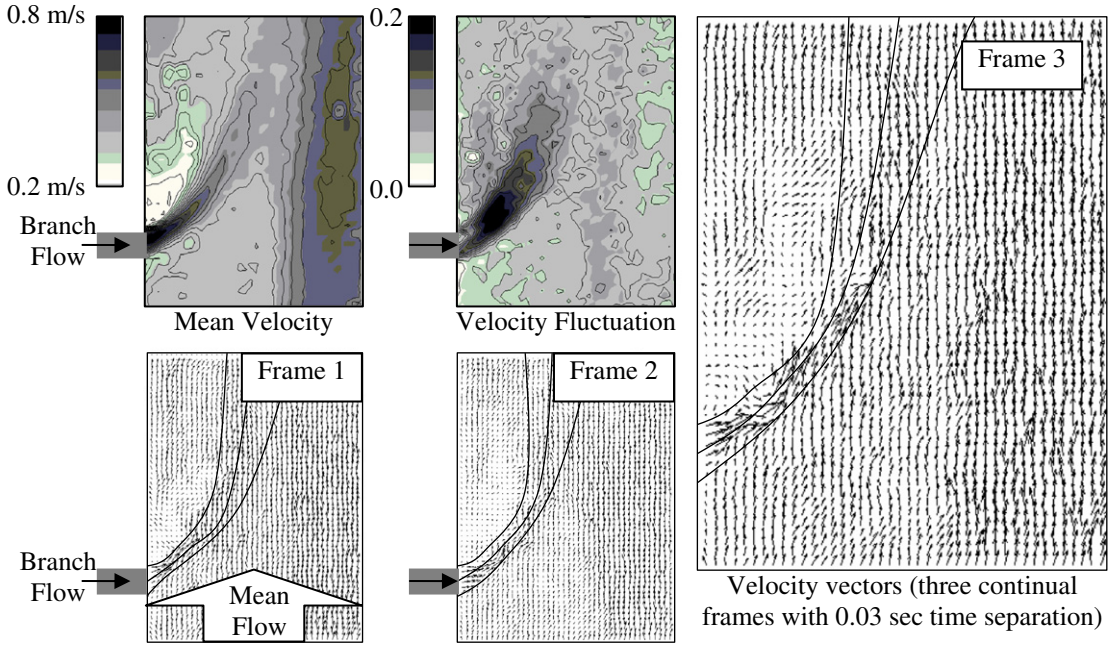

Fig. 5. Turn jet ($D_m = 108$ mm, $D_b = 15$ mm, $U_m = 0.56$ m/s, $U_b = 0.7$ m/s).

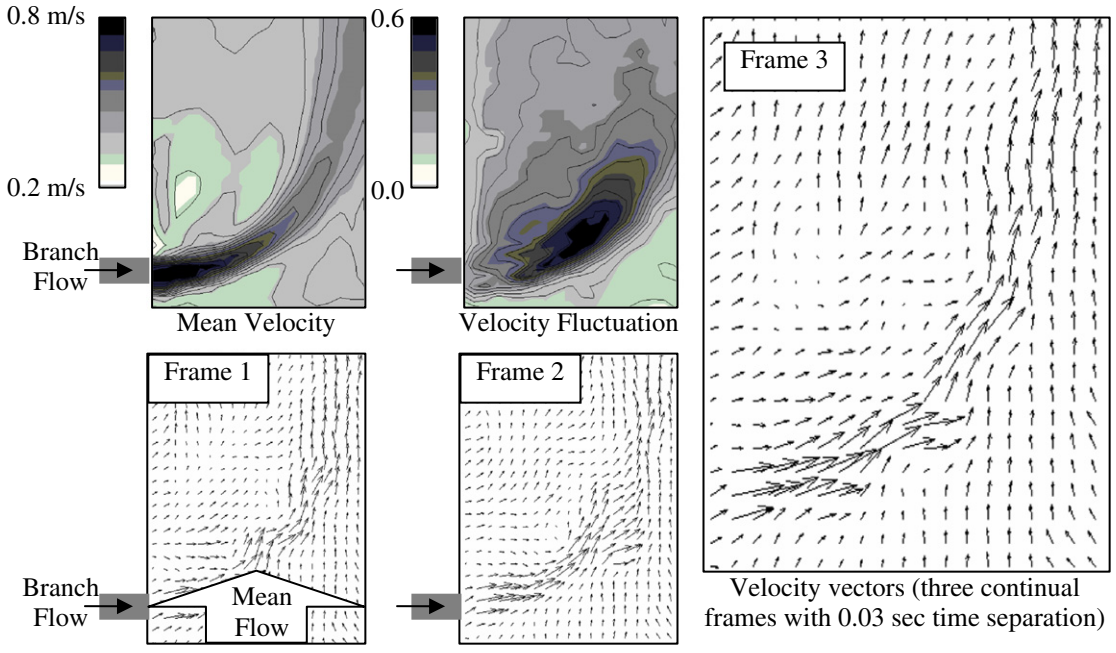

Fig. 6. Impinging jet ($D_m = 108$ mm, $D_b = 21$ mm, $U_m = 0.24$ m/s, $U_b = 0.63$ m/s).

condition was visualized at least five times (240 frames) with same experimental conditions, such as temperature (18 °C), 90-deg bend curvature ratio ($C_R = 1.4$), distance between the 90-deg bend and the branch pipe ($d/D_m = 2$), etc. By calculating the momentum ratios (M_R) of the main flow and the branch flow based on Eq. (7), a threshold for each flow pattern was defined, as shown in Table 1.

Table 1
Categorization of the branch jet in T-junction with bend upstream

	With bend
Wall jet	$90 < M_R$
Re-attached jet	$20 < M_R < 90$
Turn jet	$2.5 < M_R < 20$
Impinging jet	$M_R < 2.5$

4.2. Operating conditions

4.2.1. Momentum ratio effects

Due to many large eddies in the T-junction area with high-mixing Reynolds number ($Re = 33{,}000$–$150{,}000$), it is clear that mainly the mixing phenomena are controlled by the mechanism of these large eddies. Most of these eddies are formed by pipe geometries and an interaction between the main and branch flows [4,6]. Fig. 7 shows the maximum intensity of the velocity fluctuation near the wall of main pipe in the various momentum ratios. Velocity fluctuation has minimum intensity when the momentum ratio, is around $M_R = 2.0$. The branch pipe with a 31 mm diameter has a higher velocity fluctuation compared to the other two pipes with same momentum ratio. In this experimental condition, a larger branch pipe diameter with a constant momentum has a lower branch velocity, which means that the structure of a jet transfers to the lowest velocity ratio range with the highest velocity variation (the velocity ratios of all 31 mm branch jets are less than impinging jet velocity ratio). This also makes for higher fluctuations in 21 mm branch pipe diameter, when compared with the 15 mm pipe diameter. The velocity fluctuation at the end of chart, after $M_R = 70$, is decreasing due to the initiation of change in the jet mechanism from the re-attached jet to the wall jet with the lower fluctuation.

Only two main parameters, velocity ratio, and branch pipe diameter, can change the momentum ratio. These two parameters provide different mechanisms for the mixing phenomena, and the effects of the velocity ratio and branch pipe diameter are evaluated to consider each mechanism separately. Fig. 8 shows velocity ratio effects on the fluctuation in the different branch pipe diameters. By simply increasing the branch velocity, the velocity fluctuation decreases to the minimum condition and then begins increasing. Usually the cooling system of power plants works in the limit variation of flow rate, so that the effect of branch pipe diameter on the momentum ratio is the most important parameter for improving the operating conditions of the mixing mechanism.

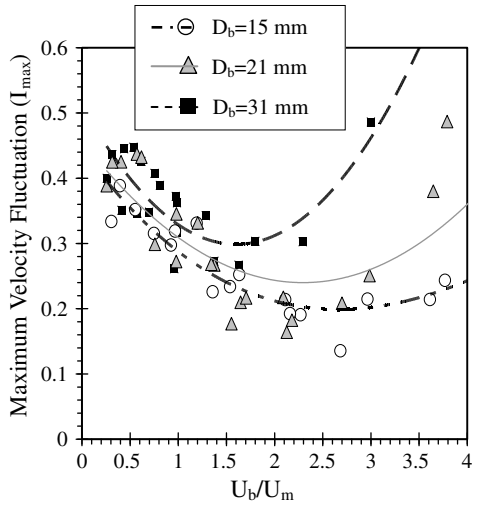

Fig. 8. Maximum velocity fluctuation near the wall in different velocity ratios.

The effects of different branch pipe diameters on the velocity fluctuations are shown in Fig. 9. Three groups are visualized (G1, G2 and G3), and each group has different branch pipe diameters and flow rates. In the group with the higher main flow rate (Q_m) and same velocity ratio occurs higher velocity fluctuations near the main pipe wall. By reducing the branch pipe diameter, if the main and branch flow rate are constant and momentum ratio is more than $M_R = 2.0$, the velocity fluctuation begins to decrease.

Since the experimental model is derived from the Phenix reactor structure design, the operating condition of Phenix is compared with other experimental conditions. It is clear that by decreasing the momentum ratio in the T-junction area of the Phenix reactor, the velocity fluctuation decreases. Two parameters have additional effects on the momentum ratio, the aforementioned pipe diameter and

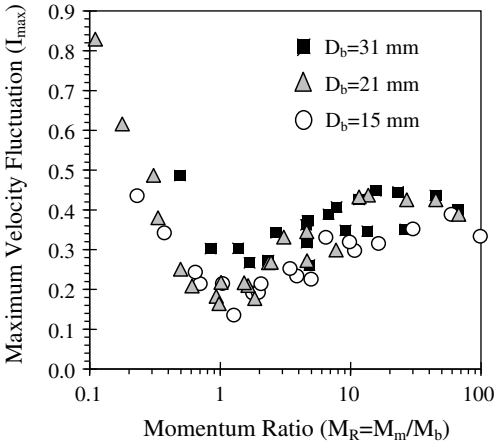

Fig. 7. Maximum intensity of the velocity fluctuation.

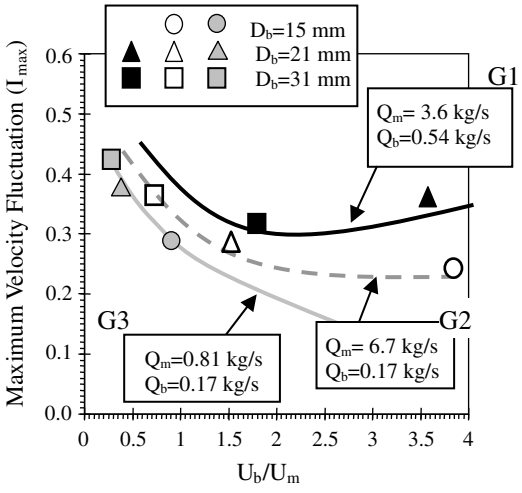

Fig. 9. Maximum velocity fluctuation near the wall with constant flow rates.

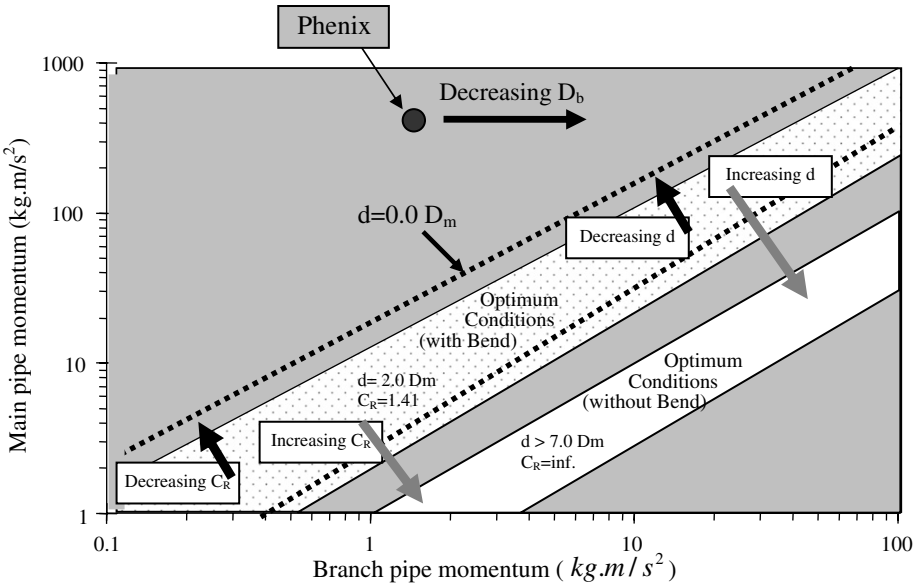

Fig. 10. Optimum operating conditions of the mixing tee with and without bend.

velocity. If we consider Phenix reactor as an example in Fig. 10, by decreasing the branch pipe diameter with a constant flow rate, the operating condition approaches optimum conditions (the optimum condition is turn jet with lowest velocity fluctuation near the main pipe wall). The momentum is dependent on the diameter, as the following equations show:

$$M_b = C \cdot \frac{1}{D_b^2}, \tag{8}$$

$$C = \frac{4Q_b^2}{\rho_b \cdot \pi} \quad Q_m \text{ and } Q_b = \text{const.}, \tag{9}$$

Q_m and Q_b are the constant flow rates in the main and branch pipes, respectively, and ρ_b is the branch flow density. It is important to know that decreasing the branch pipe diameter is helpful until the jet transfers to the optimum condition area, but after that, the pipe diameter should no longer change.

4.2.2. The effects of 90-deg bend

Given that the bend has strong effects on the fluid mixing mechanism, the two main characteristics of this bend, the curvature ratio and the axial distance between bend and branch pipe, are examined separately to distinguish the mechanism.

4.2.2.1. Axial distance effects. Fig. 11 shows the variation of the maximum vertical velocity along the axial direction of pipe, including the position of the branch pipe. The main velocity is 0.61 m/s in the pipe, with 56 mm diameters for three bends with 1, 1.5 and 2 curvature ratios. The 90-deg bend's secondary flow changes the turbulent mixing mechanism and differentiates it from the T-junction without a bend [4]. The secondary flow weakens downstream and the non-uniform axial flow congruently becomes a fully developed flow. Before this occurrence, the branch pipe was connected above the bend, and both the secondary flow and the non-uniform axial flow were still strong enough to affect the fluid mixing mechanism in the T-junction area [4].

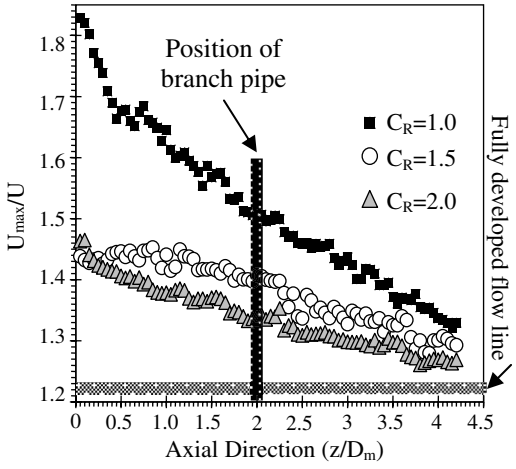

Fig. 11. Variation of the maximum axial velocity along the axial direction.

Fig. 10 also describes the optimum operating condition of the T-junction with and without bend. If the distance between the branch pipe and the bend multiplies, the optimum area narrows, thus transferring to the area with the higher momentum of branch flow and the lower momentum of main flow. After $d = 7.0D_m$ along the axial direction, the main flow acts as a fully developed flow equivalent to that without bend, so that the secondary flow and the non-uniform axial velocity are weak and ignorable. The Phenix reactor was operating out of this area in almost $2D_m$ axial direction, and by connecting the branch

pipe closer to the bend, the fluctuations near the wall decrease.

Temperature fluctuation is evaluated along the axial direction above the branch pipe near the main pipe wall as shown in Fig. 12. By using branch pipe closer to the bend, the temperature fluctuation also decreases, which means bend has positive effect to reduce the temperature fluctuation near the main pipe wall.

4.2.2.2. Curvature ratio effects. The curvature ratio has strong effects on the velocity distribution as shown in Fig. 11. The lower curvature ratio ($C_R = 1$) creates a more non-uniform velocity distribution with a strong secondary flow (Fig. 15a and b). The secondary flow in the lateral section eases the injection of the jet into the main pipe and carries two big eddies with different rotation as a twin vortex [5,6]. The energy of secondary flow dampens downstream, as shown in Fig. 13. The mean velocity is 1.15 m/s in the pipe with 56 mm diameters for three bends with 1, 1.5 and 2 curvature ratios. The secondary flow has high energy and is able deform the jet structure.

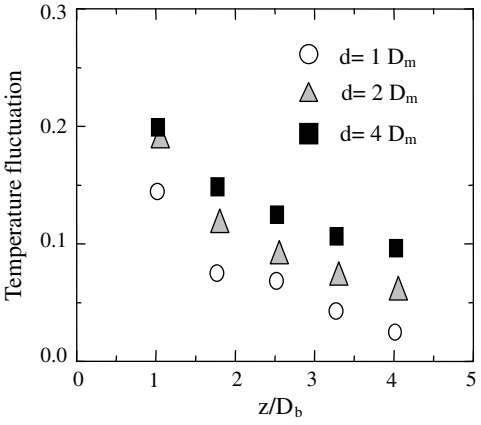

Fig. 12. Temperature fluctuations near the main pipe wall along the axial direction.

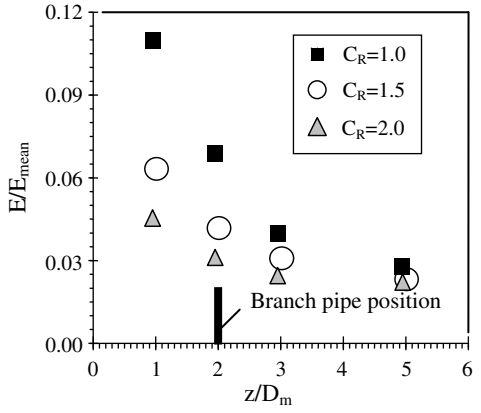

Fig. 13. Secondary flow decay energy per mean flow energy.

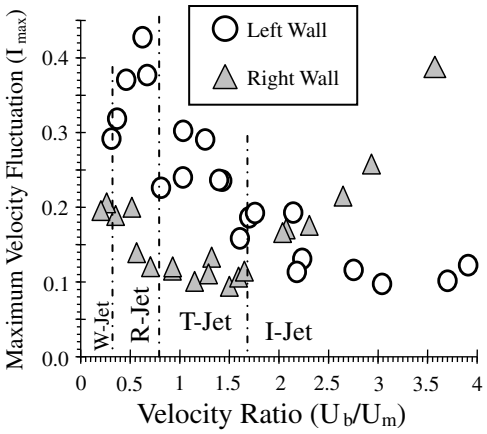

Fig. 14. Maximum intensity of the velocity fluctuation.

The secondary flow in the middle of pipe has a high velocity area and the same flow direction as the jet, see Fig. 15b. This high velocity area pushes the jet into the main pipe and the jet moves easily to the center of pipe, meaning that the jet acts here as a high velocity jet [6]. Fig. 14 shows the maximum intensity of the velocity fluctuation for the velocity ratios of each jet, such as the wall jet range (W-Jet), the re-attached jet range (R-Jet), the turn jet range (T-Jet), and the impinging jet range (I-Jet). This maximum intensity is calculated from the velocity fluctuations near the inner surface of the main pipe wall in the T-junction area. The velocity ratios in the turn jet area have the best condition with lowest fluctuations, therefore if the secondary flow is strong enough to move the jet from the wall jet range and the re-attached jet range to the turn jet range, this secondary flow is positively acting. If the opposite occurs, and this secondary flow transfers the jet from the turn jet range to the impinging range, then it is negatively acting. The secondary flow could also include a twin vortex, which are two large eddies that move downstream and produce high velocity fluctuations in the all areas with low frequency. Secondary flows with higher energy are more destructive and also help the jet to move deeper inside the pipe at the same time.

Fig. 16 shows temperature variations near the main pipe wall in T-junction area. Two bends with 1.0 and 1.41 curvature ratios are used. A smaller curvature ratio causes the lower temperature variation. By increasing the branch flow, both bends show the same distribution of temperature variation

When considering the effects of a bend to classify flow patterns with high details, the T-junction with a 90-deg bend upstream is compared to that lacking bends. The same classification of flow patterns in the T-junction area without a 90-deg bend upstream is evaluated by other research groups [9], and shown in Table 2. The 90-deg bend has strong effects on the momentum ratio range and changes the mechanism of all jets to shift them to

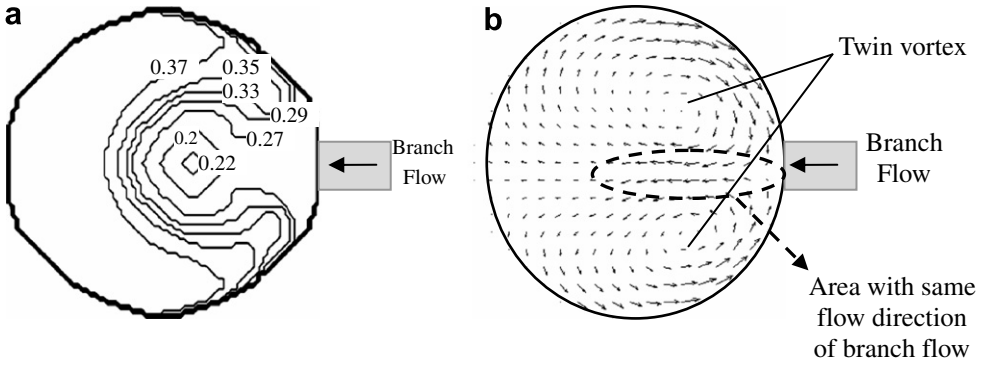

Fig. 15. Longitudinal and lateral flow with $C_R = 1.5$ and $U_m = 0.34$ m/s. (a) Longitudinal velocity contour after bend and (b) velocity vectors of the secondary flow after bend.

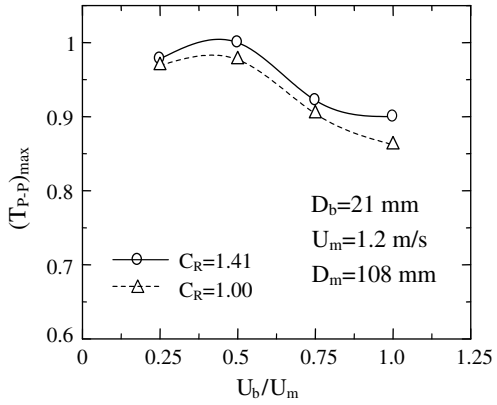

Fig. 16. Temperature variations by increasing branch flow for two bends with different curvature ratios.

the area with higher momentum ratio (almost 15 times more). In the case without bend, in Fig. 17, all boundary lines shift to the lower momentum ratios with a narrow distribution.

Table 2
Categorization of the branch jet in T-junction without the bend

	Without bend [9]
Wall jet	$4 < M_R$
Re-attached jet	$1.35 < M_R < 4$
Turn jet	$0.35 < M_R < 1.35$
Impinging jet	$M_R < 0.35$

5. Conclusion

The branch jet in the T-junction area acts as a turbulent jet in finite space. Various types of jets exist, dependent on the pipe's geometries and the physical properties of the working fluid. Momentum ratios between the main flow and the branch flow were selected to categorize different groups of branch jets based on the mechanisms and structures of each group. Finally, four groups of turbulent jets with different operating conditions in the T-junction area were introduced, such as the wall jet, re-attached jet, turn

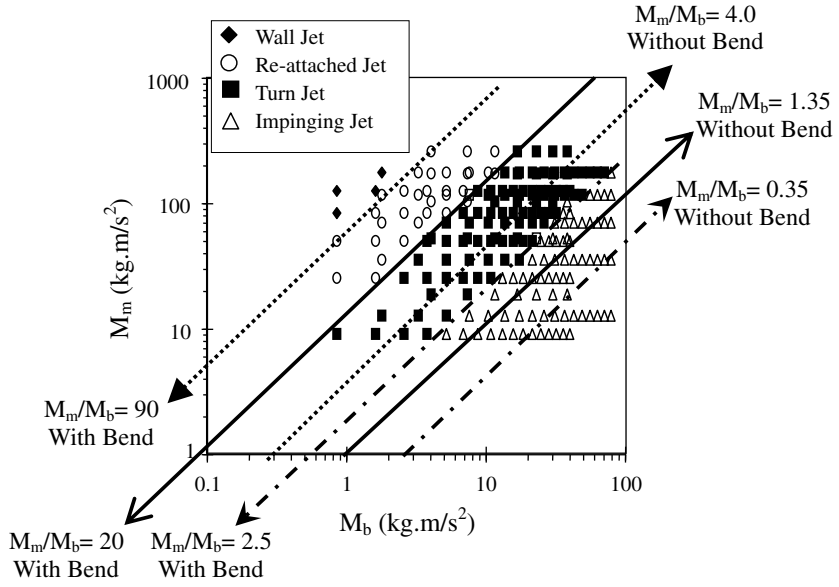

Fig. 17. Classification of fluid mixing patterns in the mixing tee with/without bend.

jet and impinging jet. The main results of the fluid mixing phenomena are listed as follows:

1. The momentum ratios of the turn jet have the lowest velocity fluctuation.
2. The flow rate of turn jet gradually transfers to the flow rate of re-attached jet with higher velocity fluctuations by increasing the momentum ratio.
3. The flow rate of turn jet sharply transfers to the flow rate of impinging jet with a much higher velocity fluctuation, by decreasing the momentum ratio.
4. The velocity and temperature fluctuations near the wall decrease by increasing the velocity ratio with a constant flow rate.
5. The velocity and temperature fluctuations near the wall decrease by decreasing the branch pipe diameter with a constant flow rate.
6. By increasing the curvature ratio of bends with a constant flow rate, the optimum operating conditions transfer to the a higher momentum ratio and narrows.
7. By connecting the branch pipe closer to the bend, the optimum operating conditions transfers to the lower momentum ratio and becomes wider.
8. The secondary flow of bend has strong effects on the fluid mixing in the T-junction and pushes the jet into a main pipe easily, which makes it act as under a higher momentum ratio without changing the flow rate.

Many different types of T-junctions are used in nuclear power plants. The temperature fluctuation in the mixing tee, which causes high cycle thermal fatigue, can be decrease more than 50% by changing simple geometries of the piping system, such as the branch pipe diameter, the distance between the bend and the branch pipe, the curvature ratio of the bend, etc. The present research is useful to assess the future design of piping systems for prolonged operation.

References

[1] C. Faidy, in: Third International Conference on Fatigue of reactor Components, EPRI-US NRC-OECD NEA, Seville, Spain, 2004.
[2] M. Tanaka, in: Proceedings of Sixth International Conference on Nuclear Thermal Hydraulic, Operation and Safety, ID: N6P334, NUTHOS-6, Nara, Japan, 2004.
[3] M. Igarashi, Study on fluid mixing phenomena for evaluation of thermal striping in a mixing tee, in: 10th International Topical Meeting on Nuclear Reactor Thermal Hydraulic, NURETH-10, Seoul, Korea, 2003.
[4] S.M. Hosseini, Experimental investigation of thermal-hydraulic characteristics at a mixing tee, in: International Heat Transfer Conference, FCV-17, Sydney, Australia, 2006.
[5] S.M. Hosseini, The three-dimensional study of flow mixing phenomenon, in: International Conference Nuclear Energy for New Europe, ID: 037, Bled, Slovenia, September 2005.
[6] S.M. Hosseini, Visualization of fluid mixing phenomenon, in: Sixth International Congress on Advances in Nuclear Power Plants, ICAPP05, ID: 5006 (R006), Seoul, Korea, May 2005.
[7] K. Yuki, in: Proceedings of the Fifth World Conference on Experimental Heat Transfer Fluid Mechanics and Thermodynamics, vol. 2, 2001, pp. 1573–1578.
[8] K. Yuki, in: Proceedings of the 15th International Conference on Nuclear Thermal Hydraulic, Operation and Safety (NUTHOS-6), ID: N6P082, Nara, Japan, 2004.
[9] M. Igarashi, in: Proceedings of the 10th International Conference on Nuclear Engineering, ICONE10-22255, Arlington, VA, 2002.